Electronic Supplementary Material

A colorimetric sensor with dual-ratio and dual-mode for detection of nicotine in tobacco samples

Jian Li,[a] Pengcheng Liang,[a] Huijuan Song,[a] Xia Yu,[a] Shiyu Hu,*[a] Jiaqi Wang,[a] Cong Cheng,[a] Yan Zhao*[b] and Zhaohong Su*[a]

[a] College of Chemistry and Materials Science, College of Agronomy, Hunan Agricultural University, Changsha 410128, PR China.

[b] College of Chemistry and Chemical Engineering, Hunan University, Changsha 410082, China.

*Corresponding author. Tel.: +86 731 84618071; fax: +86 731 84618071.

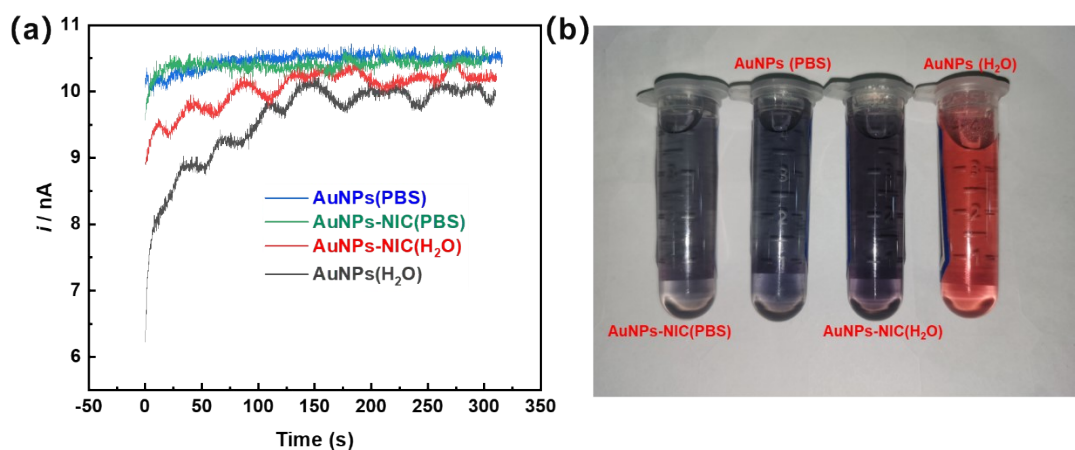E–mail address: hushiyu@stu.hunau.edu.cn; zhaoyan@hnu.edu.cn; zhaohongsu@hunau.edu.cn

Fig. S1. (a) I-t curves and (b) physical images of AuNPs under different conditions.

As can be seen from Fig. S1, the i-t curves of AuNPs-NIC and AuNPs in H_2O show wavy fluctuations, while in PBS they are very stable, and the current response in PBS is higher than that in H_2O. This phenomenon may be related to the surface charge and solution conductivity of AuNPs-NIC. AuNPs-NIC is a nanocomposite composed of AuNPs and nicotinamide (NIC), which has a certain surface charge that can affect its adsorption and desorption on the electrode surface[1]. In H_2O, the surface charge of AuNPs-NIC is weak, so the adsorption and desorption on the electrode surface are easily influenced by the electric field, resulting in a wavy fluctuation of the i-t curve[2]. In PBS, the phosphate ions in PBS compete with sodium citrate for the surface sites, which causes the aggregation of AuNPs-NIC and AuNPs, and also modulates the surface charge of AuNPs, and increases the conductivity of the solution, resulting in faster and stronger current response. Therefore, in PBS, the i-t curve of AuNPs-NIC is more stable, and the current response is higher than that in H_2O.
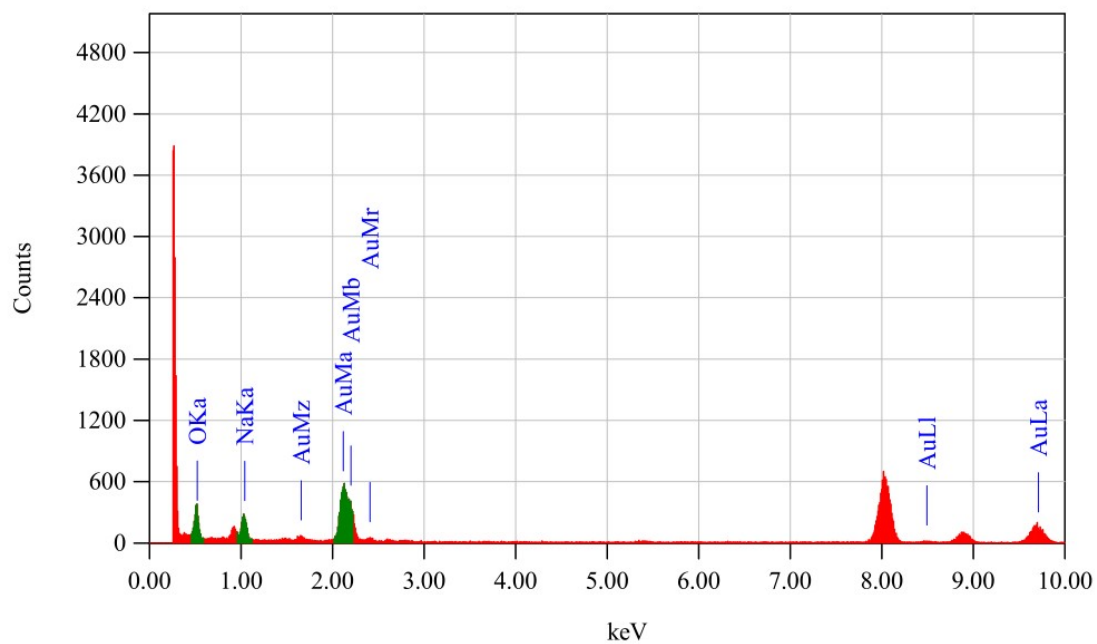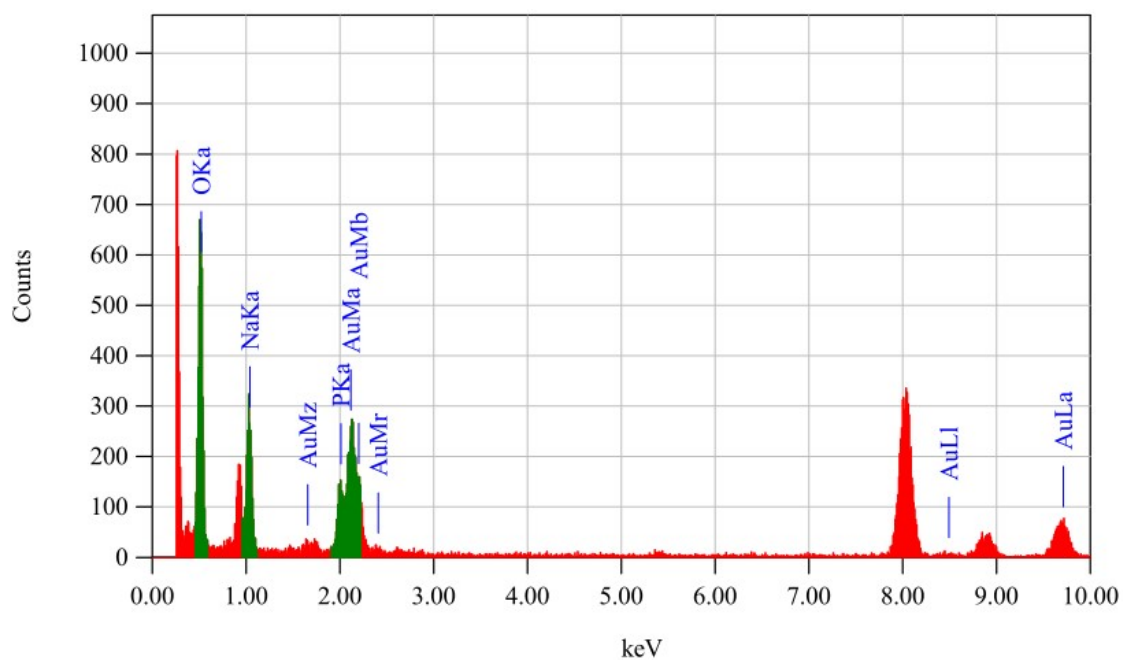
Fig. S2. Energy spectrum of AuNPs.

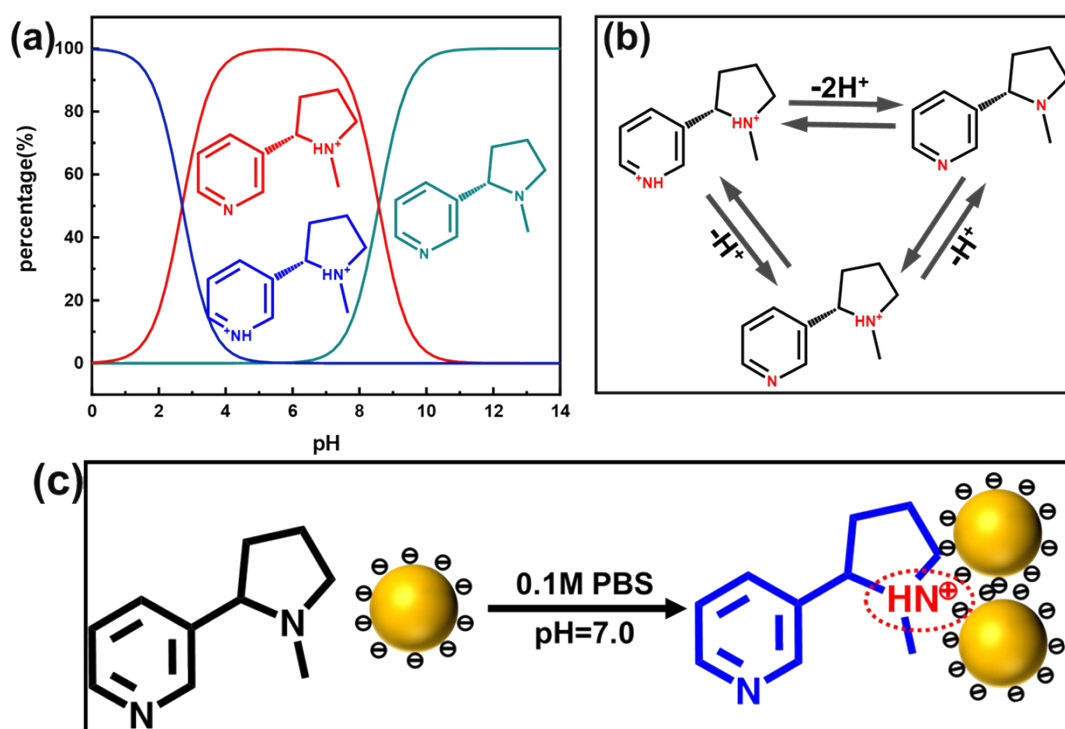

Fig. S3. Energy spectrum of AuNPs-NIC.

Fig. S4. (a) pK$_a$ and (b) morphological changes of NIC. (c) Possible mechanism diagram of AuNPs and NIC interaction.
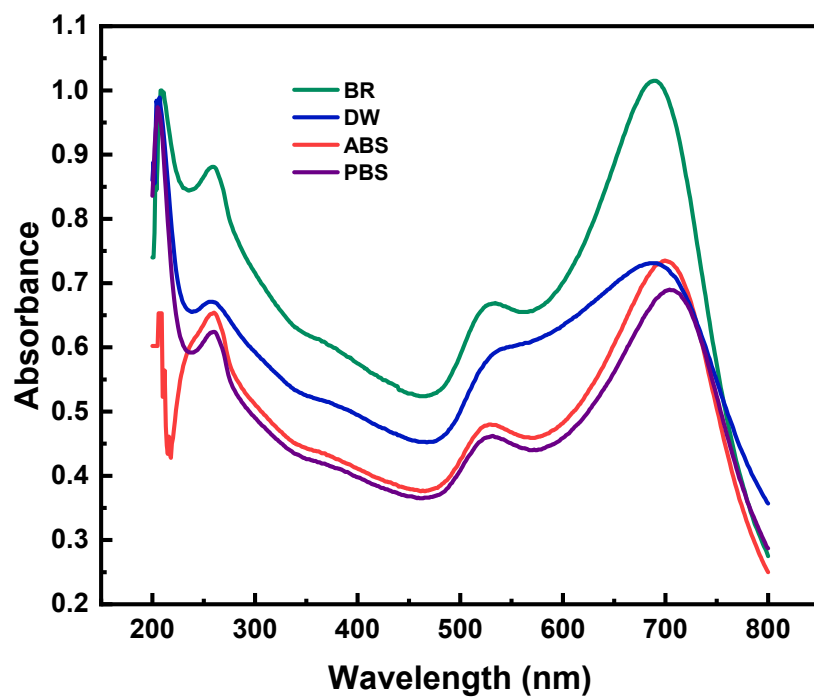

Fig. S5. UV-vis response of AuNPs-NIC in different buffer solutions. All buffer solutions have concentrations of 0.1 M and pH values of 7.

Fig. S5 shows the UV-Vis response of AuNPs-NIC in DW, PBS, BR, and ABS with pH 7, respectively. It can be seen that the anions in other buffer solutions also have a certain promoting effect on the competition of NIC for the surface sites of AuNPs, which further confirms the typicality of this mechanism, which can be applied to more anions.
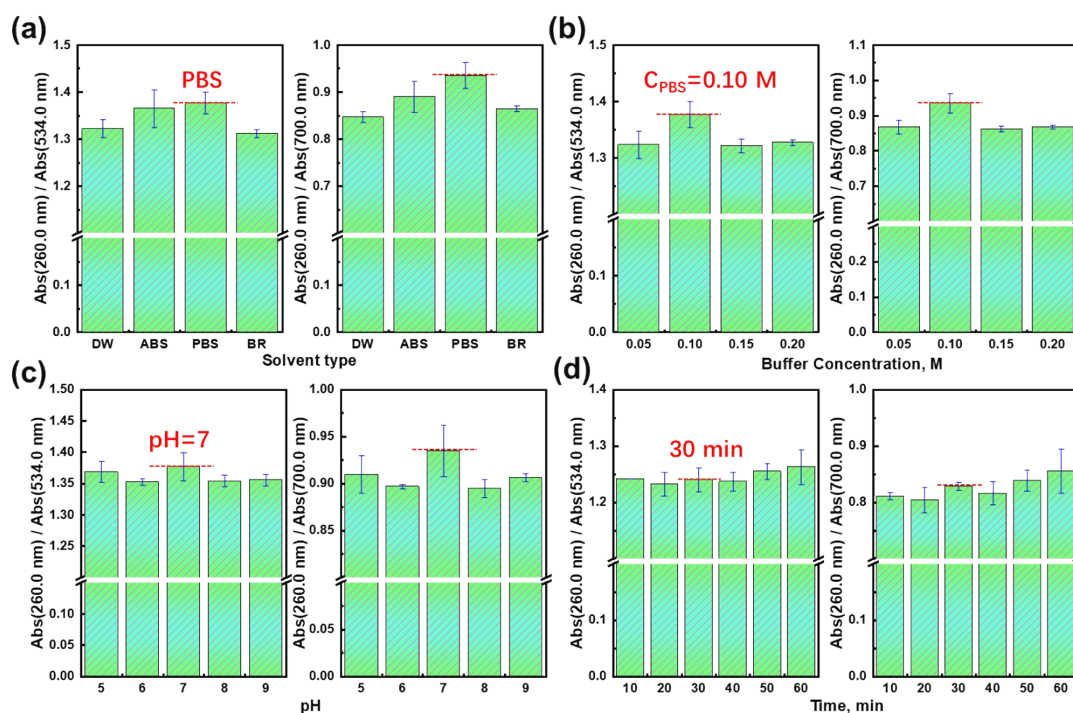

Fig. S6. Optimization parameters for NIC analysis based on dual ratio AuNPs signals: (a) solvent type, (b) buffer concentration, (c) pH, and (d) reaction time.

Based on the premise of NIC concentration of 40 μM, systematic experimental analysis was conducted on factors such as solvent type, buffer concentration, pH and reaction time between NIC and AuNPs. First, different types of solvents, such as phosphate buffer solution (PBS), distilled water (DW), acetic acid buffer (ABS) and Britton-Robinson (BR) buffer solution were selected to compare their effects on the detection of NIC. The experimental results show that the detection sensitivity and

accuracy of NIC in different buffers are different. Among them, phosphate buffer has the best detection effect (Fig. S6a), and the subsequent experiments are carried out using this solvent. In addition, from the UV-vis spectra of different buffer solutions (Fig. S5), it can be seen that other buffer solutions containing anions can also produce the same agglomeration longitudinal LSPR peak as PBS, which further indicates that anions X^- in the possible mechanism diagram of Fig. 1c include most other anions similar to phosphate anions. Second, the effect of buffer concentration on the detection of NIC was investigated. By comparing the phosphate buffers with concentrations ranging from 0.05 μM to 0.20 μM, it is found that the buffer with a concentration of 0.10 μM has a significantly higher absorption rate (Fig. S6b). Therefore, 0.10 μM is chosen as the optimal buffer concentration. In addition, the pH value of the buffer was adjusted experimentally, and the absorption ratio of the dual signal was tested using a pH range of 5~9. The results show that the change of pH value has some influence on the detection result of NIC. When the pH was 7, the absorption ratio is the highest. The ratio of absorption peaks is highest when pH is 7, at which point HPO2-4 is the dominant phosphate anion in PBS, indicating that it has a stronger ability to assist NIC in competing for the surface sites of AuNPs. However, too acidic or too alkaline reduces the absorption ratio of the detection signal of NIC (Fig. S6c). This suggested that neutral medium is suitable for analysis based on AuNPs, because the stability of AuNPs is affected by acidic and/or alkaline medium [3]. Finally, in order to study the influence of the interaction time between NIC and AuNPs on the detection result, the absorption ratio was measured in the range of

10~60 min. According to the experimental results analysis, it is found that when optimizing the NIC spectrophotometry based on AuNPs, the reaction time of 30 min has a local optimum within 10~40 min. However, better detection results are obtained at 50 min and 60 min (Fig. S6d). This phenomenon might be due to the fact that the reaction reached a local optimum at 30 min. But at longer reaction times, NIC can react more fully with AuNPs, resulting in further improvement of detection sensitivity and accuracy. In addition, since the choice of reaction time also needed to consider the rapid detection occasions in practical applications, too long reaction time increases its cost. Therefore, 30 min is chosen as the optimal reaction time.
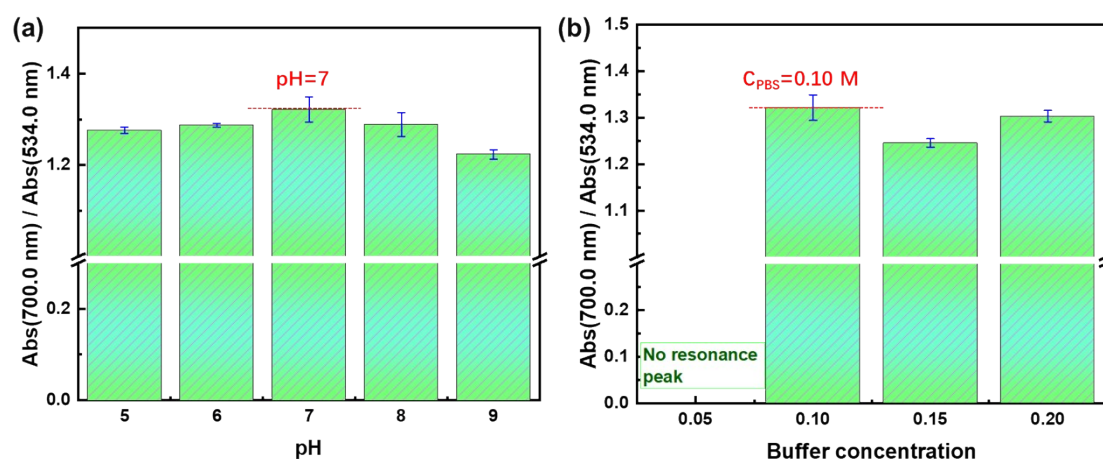

Fig. S7. The effect of (a)buffer pH and (b)ionic strength the AuNPs.

Fig. S7 indirectly reflects the aggregation state of AuNPs by comparing the ratio of the two resonance peaks under different pH and ionic strength. It can be seen that when the pH of PBS is 7 and the ionic concentration is 0.1M, the ratio of the two peaks is the highest, which means that the aggregation strength of AuNPs is the strongest at this time. This result is also consistent with Fig. S6, and combined with the explanation of the effect of aggregation on LSPR in Fig. 3, it can be concluded

that phosphate ions cause AuNPs to aggregate, and after the electron layer around them rearranges, they attract NIC. The higher the degree of aggregation of AuNPs, the denser the distribution of the electron layer, and the stronger the attraction to NIC, thus enhancing the detection signal.
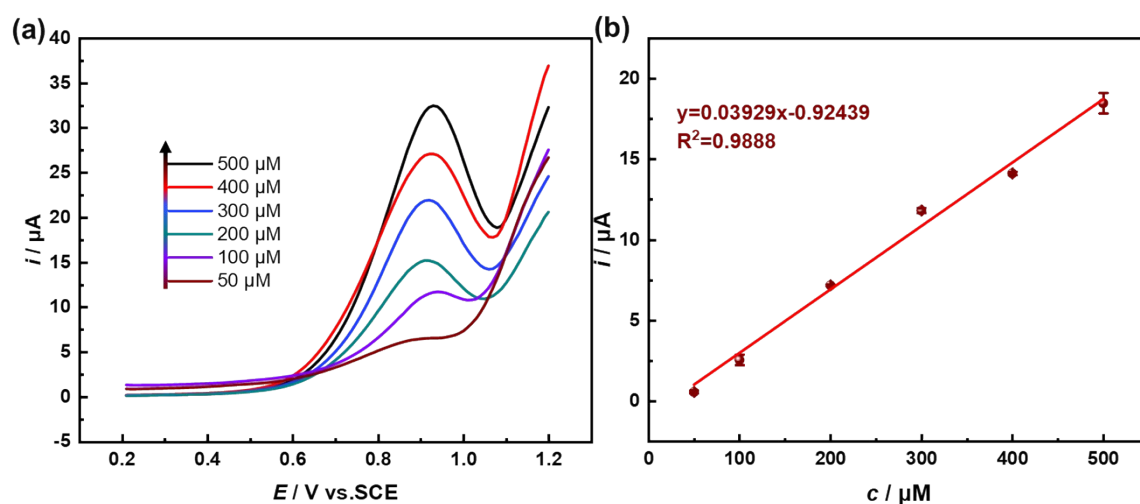

Fig. S8. (a) SWV curves of different concentrations of NIC. The linear correlation curve of peak currents vs concentration of NIC.

To further verify the reliability of this method, we applied the conventional electrochemical method to test the real samples. Fig. S8a displays the SWV response of the bare SPCE in various concentrations of NIC solution, and Fig. S8b presents the calibration curve, which yields the calibration equation as y = 0.03929x - 0.92439 (R^2=0.9888). Linear range is 50-500 μM, LOD is calculated to be 2.77 μM, and LOQ is 9.24 μM, and. The data of the real samples measured by the SPCE is given in Table 1.
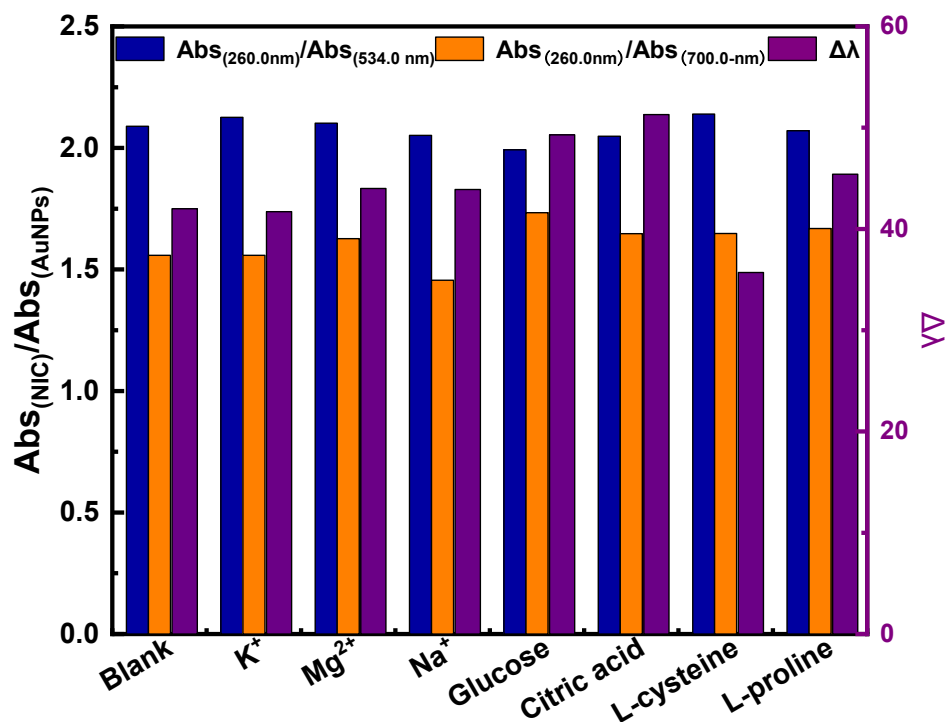
Fig. S9. (a) The absorbance ratio and wavelength response of 100 μM AuNPs in 0.1M PBS containing 40 μM NIC (pH=7) with different interfering substances. The ion concentrations of K^+, Mg^{2+}, and Na^+ are 1 mM, and the concentrations of glucose, citric acid, L-cysteine, and L-proline are 5 mM.
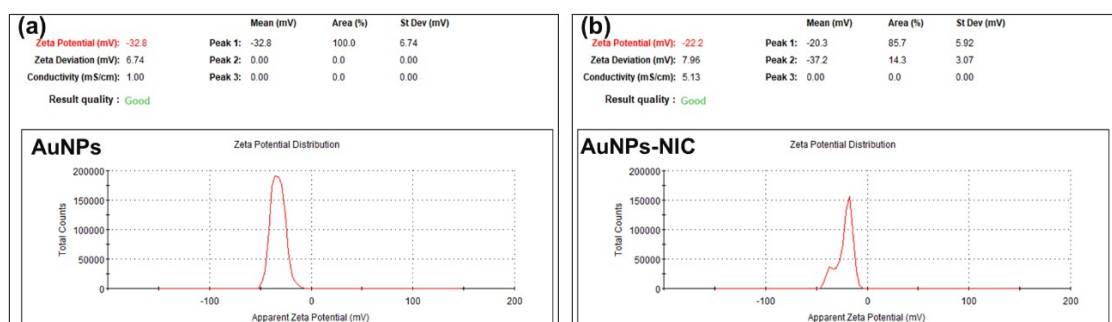

Fig. S10. One of zeta potential of (a) AuNPs and (b) AuNPs-NIC.

Table S1. NIC related data table.

Property	Value
Chemical formula	$C_{10}H_{14}N_2$
UV absorption peak position	260 nm
Molecular weight	162.23 g/mol
Optical isomers	2
pK_a	2.7 and 8.5
Physical state	Oily liquid
Solubility	Soluble in water and ethanol
Density	1.01 g/cm^3
Main metabolite	Cotinine
Route of excretion	Urine

Table S2. The LUMO-HOMO energy level orbitals and the optimization parameters of the UV-vis spectrum of the NIC molecule.

Optimization object	Step	Job Type	Method	Basis Set	Solvation
LUMO-HOMO energy level orbitals	1	Frequency	Groud State~ DFT~ Restrictrd-B3LYP	6-311g(d)	None
	2	Energy	Groud State~ DFT~ Restrictrd~ B3LYP	6-311g(d,p)	None
	3	Energy	TD-SCF~ Hartree-Fock~ Default Spin	6-311g	None
UV-vis spectrum	1	Frequency	Groud State~ DFT~ Restrictrd-B3LYP	6-311+g(2d,p)	Read checkpoint filea
	2	Energy	TD-SCF~ DFT~ Restrictrd~ B3LYP	6-311+g(2d,p)	Water

Table S3. Comparison of different probes for NIC spectrophotometric detection.

Signal probe	Linear rang/ μM	LOD/ μM	Sample	pH	Buffer solution	References
Molecularly imprinted polymers	1.1-60	1.1	urine	7.5	0.01 M PBS	[4]
Cerric sulphate	1.8–36.0	0.32	cigarettes, urine,	7.0	0.1 M PBS	[5]
Molecularly imprinted polymers /ZnO	0.006–1.54	0.002	cigarettes and cigar	7.5	0.1 M BR	[6]
Alizarin Red S	0-2×10^4	425.0	E-liquid	—	1 : 1 propylene glycol and glycerin	[7]
Methyl Orange dye	0.61–24.0	0.36	cigarette tobacco	—	—	[8]
Carbon nanotube/zinc oxide nanocomposite	1.0–150 μg/L	0.3 μg/L	seawater, human plasma and cigarette.	—	—	[9]
AuNPs AgNPs	0.001–0.3 0.10–5.0	0.001 0.09	tobacco, simulated blood plasma, and simulated urine	7.0	0.1 M PBS	[10]
AuNPs	5-500	2.48 1.63 1.34	cigarette tobacco	7.0	0.1 M PBS	This work

References (only for Electronic Supplementary Material)

1. K. Saito, K. McGehee and Y. Norikane, *Nanoscale Advances*, 2021, **3**, 3272-3278.

2. C. Hou, Q. Luo, Y. He and H. Zhang, *J. Appl. Electrochem.*, 2021, **51**, 1721-1730.

3. Y. Gao, Y. Wu and J. Di, *Spectrochimica Acta Part A: Molecular and Biomolecular Spectroscopy*, 2017, **173**, 207-212.

4. E. C. Figueiredo, D. M. de Oliveira, M. E. P. B. de Siqueira and M. A. Z. Arruda, *Anal. Chim. Acta*, 2009, **635**, 102-107.

5. H. A. Omara and H. M. Younis, *Sirte University Scientific Journal*, 2015, **5**, 65-74.

6. S. H. Hashemi and F. Keykha, *Anal. Methods*, 2019, **11**, 5405-5412.

7. R. Jerome and A. K. Sundramoorthy, *Anal. Chim. Acta*, 2020, **1132**, 110-120.

8. Y.-J. Huang, Q.-X. Deng, H.-Q. Lan, Z.-Z. Fang, H. Chen, Y. Lin, H.-C. Xu, T. D. James and W. Xie, *Anal. Methods*, 2020, **12**, 193-199.

9. S. H. Hashemi and N. Naruie, *J. Anal. Chem.*, 2021, **76**, 563-572.

10. Z. O. Erdogan and H. Balci, *Spectrochimica Acta Part A: Molecular and Biomolecular Spectroscopy*, 2023, **285**, 121853.